

Dynamic responses of structures with sliding base

Jiin-Song Tsai† and Wen-Ching Wang‡

Department of Civil Engineering, National Cheng Kung University, Tainan 70101, Taiwan, R.O.C.

Abstract. This paper presents dynamic responses of structures with sliding base which limits the translation of external loads from ground excitation. A discrete element model based on the discontinuous deformation analysis method is proposed to study this sliding boundary problem. The sliding base is simulated using sets of fictitious contact springs along the sliding interface. The set of contact spring is to translate friction force from ground to superstructure. Validity of the proposed model is examined by the closed-form solutions of an idealized mass-spring structural model subjected to harmonic ground excitation. This model is also applied to a problem of a three-story structural model subjected to the ground excitation of 1940 El Centro earthquake. Analyses of both sliding-base and fixed-base conditions are performed as comparisons. This study shows that using this model can simulate the dynamic response of a sliding structure with frictional cut-off quite accurately. Results reveal that lowering the frictional coefficient of the sliding joint will reduce the peak responses. The structure responses in little deformation, but it displaces at the end of excitation.

Key Words: sliding structure; sliding boundary problem; discontinuous deformation analysis.

1. Introduction

In attempts to mitigate the earthquake hazards on buildings, the concept of decoupling the structures, and/or its contents, from potentially damaging earthquake induced ground motion has been adopted in recent seismic resistance practices. Building with a sliding joint underneath is probably the simplest type of these practices. The sliding joint offers a discontinuity to the ground motion propagation and dissipates energy through horizontal frictional force. In practice, a teflon coated surface or a layer of sand used in this joint would essentially provide a pure-friction sliding base (Fig. 1). This idea, although some experiments may have shown its attractive characteristics, has not been sufficient proven quantitatively to merge into conventional and established design procedures. In fact, the responses of various sliding structures have not been thoroughly understood yet. Since the seismic design is a concern of life safety through the uncertainty study, engineering applications, such as structures with sliding base, must be subjected to intensive studies. This conceptually simple idea of sliding base obviously requires much more research to make it applicable.

Responses of sliding structures subjected to harmonic ground motion have been studied theoretically by Westermo and Udawadia (1983) and Mostaghel, *et al.* (1983a). Experiments of a model on a shaking table subjected to sinusoidal excitation have been carried out by Li, *et al.* (1989). The effectiveness of sliding supports in mitigating structures damage from earthquakes has been

† Associate Professor

‡ Ph.D. Student

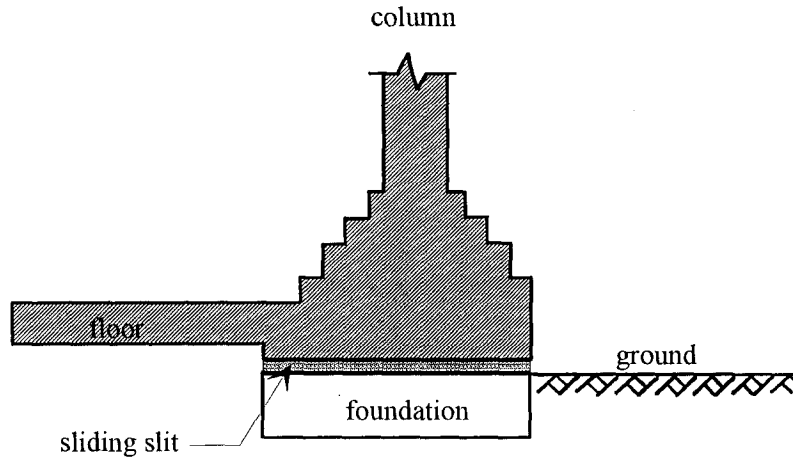


Fig. 1 Frictional isolation base.

investigated by Mostaghel and Tanbakuchi (1983b). In these early studies, a mathematical mass-spring model (Appendix I) with two degrees of freedom has frequently been adopted for the simulation of sliding structure. The mass-spring model is basically in the form of lumped masses with springs to represent building of shear resistant type. Both the superstructure and the sliding base are represented as two single degree-of-freedom (SDOF). Adopting the similar mass-spring concept, Yang, *et al.* (1990) has proposed a multi-degree-of-freedom (MDOF) model.

To further explore the applicability of the sliding base in the seismic design, this paper presents dynamic response analyses of the sliding structures using the discrete element model. This model has similar attraction of the finite element method to approximate the geometry of structure using many individual elements or "blocks". It is applicable to model structures besides those of shear resistant type, and has better applicability than the existing models mentioned above. In the present study, analyses are performed for comparisons using two different models, including a mass-spring model and a discrete element model.

The sliding joint is simulated as the inherent discontinuity surface between discrete elements. Frictional effect along the sliding joint is modeled as the contact described by Coulomb frictional law, which is independent of pressure and velocity, and no difference is expected between the coefficients of static and dynamic friction. The commonly accepted fictitious-spring (or penalty) concept is adopted to model the translation of friction force, which is simulated using a pair of orthogonal contact-springs between elements.

In the discrete element model, the input and solution of a process occurred within a time domain are treated as a series of discrete events and the governing equations of motion are solved incrementally. Hence, virtually no restraint needs to be placed on the type of ground motion for the sliding base problem. Theoretical formulations of the proposed model are based on the discontinuous deformation analysis method (Shi and Goodman 1984) and are described in the following section.

2. Theoretical formulations

In the mechanic analysis, the sliding boundary condition of the structure with a sliding base

is a special problem of interest. In the present study, this problem is analyzed using a discrete element model. The adopted discrete element model meshes the configuration of structure similarly as finite element model does, except the introduction of discontinuous interfaces (or sliding joints) between elements. The following paragraphs describe concept and formulations of the discontinuous deformation analysis method. Simulation of the sliding joint for dynamic contact interaction is also included.

For last two decades, many efforts have been spent on computational mechanics for the frictional contact problem (e.g., Cundall and Strack 1983 and Walton 1993). In general, two methodologies, the force method and the displacement method, are used. Based on the force method, Cundall (1971) has introduced the distinct element method for the analyses of the mechanical behavior of discrete materials and Goodman, *et al.* (1968) has proposed a joint element for solving rock discontinuity problems. Using the displacement method, the discontinuous deformation analysis (DDA) has been proposed by Shi and Goodman (1984). This method is mainly used for solving rock mechanics problems. In the present paper, it is the first time that the DDA method is applied for solving the problem of sliding-base structure. In the following, theoretical bases of this method and some enhancements for the application of sliding structure analysis are described.

Being a displacement method, the DDA can be treated as a generalization of the finite element method. The discrete element (or block) used in the DDA is assumed to be constant stress and strain. Displacement (u, v) of any point (x, y) within an element is represented by six variables and formulated as a first order approximation form of

$$\begin{pmatrix} u \\ v \end{pmatrix} = \begin{pmatrix} 1 & 0 & -(y-y_0) & (x-x_0) & 0 & (y-y_0)/2 \\ 0 & 1 & (x-x_0) & 0 & (y-y_0) & (x-x_0)/2 \end{pmatrix} \begin{pmatrix} u_0 \\ v_0 \\ r_0 \\ \varepsilon_x \\ \varepsilon_y \\ \gamma_{xy} \end{pmatrix} \quad (1)$$

where (u_0, v_0) is the displacement of the center point (x_0, y_0) of an element; r_0 is the rotation angle and $\varepsilon_x, \varepsilon_y, \gamma_{xy}$ are two axial and the shear strains. Similar to the nodal point in a finite element mesh, the center (x_0, y_0) of each discrete element has six degrees of freedom. For a system of n discrete elements, the global simultaneous equilibrium equations are as

$$\begin{bmatrix} K_{11} & K_{12} & \cdot & \cdot & \cdot & K_{1n} \\ K_{21} & K_{22} & \cdot & \cdot & \cdot & \cdot \\ K_{31} & \cdot & \cdot & \cdot & \cdot & \cdot \\ \cdot & \cdot & \cdot & \cdot & \cdot & \cdot \\ \cdot & \cdot & \cdot & \cdot & \cdot & K_{n-1n} \\ K_{n1} & \cdot & \cdot & \cdot & K_{nn-1} & K_{nn} \end{bmatrix} \begin{pmatrix} D_1 \\ D_2 \\ D_3 \\ D_4 \\ D_5 \\ D_6 \end{pmatrix} = \begin{pmatrix} F_1 \\ F_2 \\ F_3 \\ F_4 \\ F_5 \\ F_6 \end{pmatrix} \quad (2)$$

Each K_{ij} in Eq. (2) is a 6×6 submatrix which represents the stiffness between block i and j . Submatrix K_{ii} depends on the material properties of block i . Submatrices D_i and F_i are both 6×1 and are the deformation variables and the loadings, respectively.

The frictional contact is represented using a pair of stiff springs (a normal and a shear springs) along the sliding interface. The contact between two individual elements is decomposed as a normal component R_n and a shear component R_s . The transition of the sliding and non-sliding

phases in the DDA method is governed by the Mohr-Coulomb criteria. Once the R_s is greater than the friction defined by Coulomb's law, sliding occurs.

$$R_s \geq \rho R_n = R_n \tan \theta \quad (3)$$

The dynamic frictional force in sliding phase is equal to the product of the frictional coefficient (ρ) and the normal contact force. The right hand side of Eq. (3) is the resistance of Coulomb's friction, i.e., θ is the frictional angle of contact interface. Kinetic energy of the sliding block element dissipates along the contact interface. The static frictional force in the non-sliding phase is equal to the shear spring force. Using a large spring constant, i.e., a hundred times the value of Young's modulus of discrete element, the elongation of the stiff spring along the sliding interface will remain negligible in the non-sliding phase.

In the present analyses, the ground excitation is introduced in the horizontal direction. Seismic loading is exerted onto the structural system through a large ground block underneath (Fig. 2). This loading is in the form of the inertia force of the ground block as an acceleration time history. By solving the problem incrementally, the inertia force $f_x(t_i)$ of the ground block (m_g) at time step t_i is represented as

$$f_x(t_i) = m_g \ddot{u}_0(t_i) \quad (4)$$

where m_g is a chosen large mass to represent the ground and, $\ddot{u}_0(t_i)$ is constant acceleration within time step i .

In order to mesh a larger piece using the adopted discrete elements, the connection between elements is accomplished using bolt and connection elements. The usage of bolt element is the simplest way to allow tension in-between the discrete elements. If $P_i(u_i, v_i)$ and $Q_j(u_j, v_j)$ are displacement vectors of the two ends of a bolt which connects two different elements i and j . The strain energy of the bolt is expressed as

$$\pi_b = \frac{1}{2} k \{ [(u_j - u_i) + u]^2 + [(v_j - v_i) + v]^2 \} \quad (5)$$

where k is the spring constant of the bolt, and u and v are the two relative displacement components of P_i and Q_j at previous time step as the Eq. (2) is solved incrementally. The stiffness matrix and the force vector of the bolt can be derived through minimization of total potential energy of the Eq. (5) and should be added into the global stiffness matrix and the global force vector in the Eq. (2).

The connection element is a constant strain triangular element which has nodal points located in two or three different discrete elements. Through the procedure of minimizing total potential strain energy, the stiffness matrix and the force vector of the connection element can also be added into the global stiffness matrix and the global force vector in the Eq. (2). In the current practices, four triangular elements are used for each connection in the numerical model. The strain energy for a single element is

$$\pi_e = \frac{1}{2} \int_0^{L_1} \int_0^{L_2} [\epsilon_x \epsilon_y \gamma_{xy}] [E] \left\{ \begin{matrix} \epsilon_x \\ \epsilon_y \\ \gamma_{xy} \end{matrix} \right\} J dL_1 dL_2 \quad (6)$$

where L_1 and L_2 are the shape functions used in the constant strain element. J is defined as

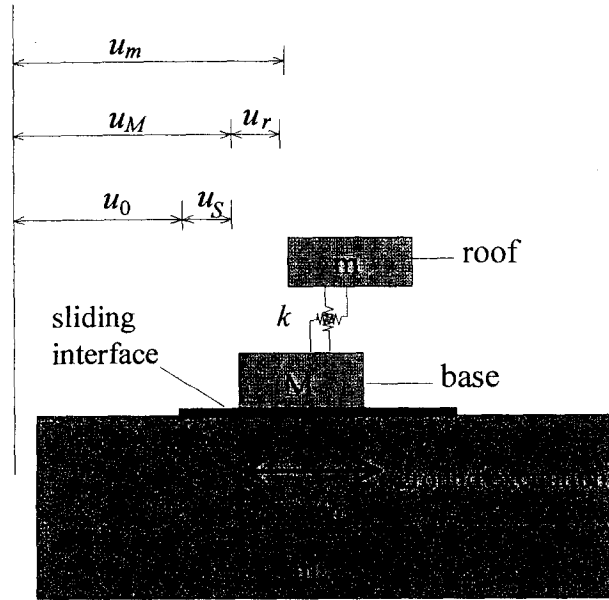


Fig. 2 Simple two-element model.

$$J = \begin{vmatrix} J_{11} & J_{12} \\ J_{21} & J_{22} \end{vmatrix} \quad (7)$$

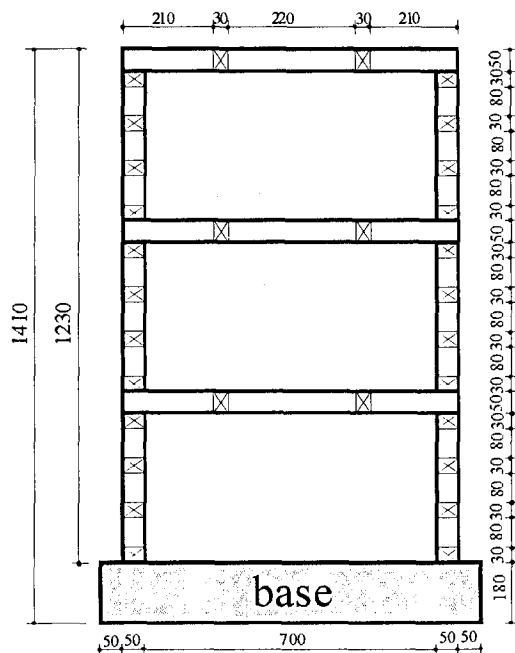
in which $J_{11}=x_1-x_3$, $J_{12}=y_1-y_3$, $J_{21}=x_2-x_3$, $J_{22}=y_2-y_3$ and (x_1, y_1) , (x_2, y_2) , (x_3, y_3) are coordinates of the nodal points of the connection element.

3. Numerical results

In this section, numerical analyses to describe the dynamic responses of structures with sliding base include a simple two-element problem (Fig. 2) and a three-story-structure problem (Fig. 3). Validity and accuracy of the DDA results are examined first using the simple two-element problem. Analytical solutions of this problem obtained using the mass-spring model are taken as the benchmarks. In the present study, material damping is not of concern. Parameters adopted for the computations are

- (1) natural frequency of the system $\omega_n=1$ Hz;
- (2) frequency ratios for the harmonic ground excitation $\Omega/\omega_n=0.1\sim 10.0$;
- (3) amplitude of the ground acceleration $a_{max}=0.3$ g;
- (4) mass ratios of the two-element system $\alpha=m/(M+m)=0.1, 0.5, 0.9$;
- (5) frictional coefficients $\rho=0.01, 0.05, 0.1, 0.25$;
- (6) duration of excitation=100 seconds (100 cycles).

Computed results of both the analytical solutions and the DDA results for the two-element system simulation are shown in Figs. 4 to 9. With different mass ratio α , each figure of Figs. 4, 6 and 8 contains the comparisons of two different measurements: (a) the maximum relative displacement between the base and the ground $|u_s|_{max}/D$ and (b) the maximum relative displacement between the roof and the base $|u_r|_{max}/D$. These measurements are normalized using a





unit:cm  connection elements
 discrete elements

Fig. 3 The three-story-building model.

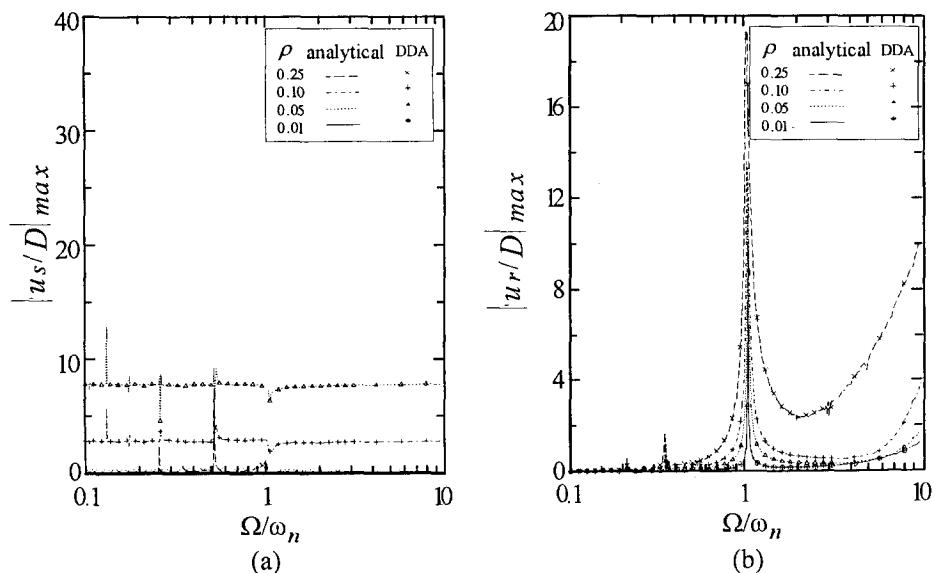


Fig. 4 Comparisons of analytical and numerical solutions for $\alpha=0.1$. (a) the maximum relative displacement between the base and the ground. (b) the maximum relative displacement between the roof and the base.

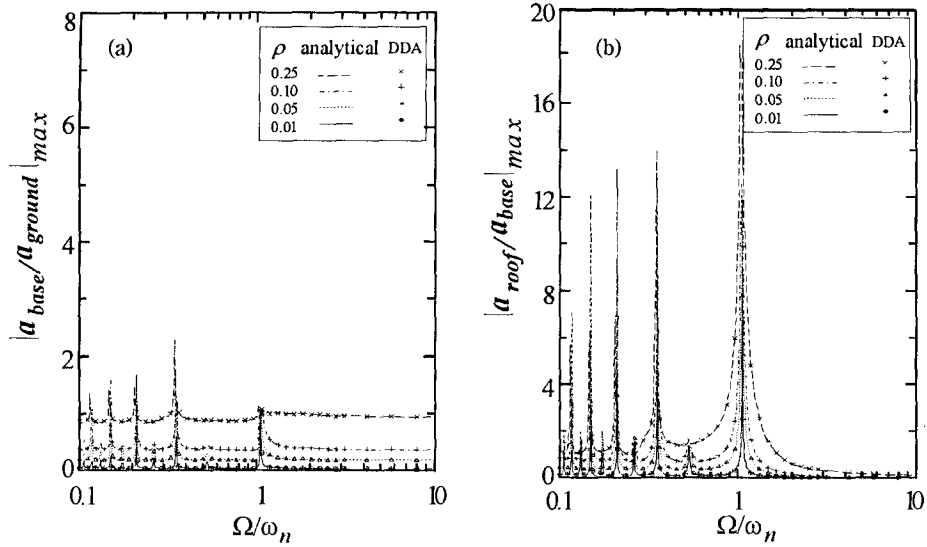


Fig. 5 Comparisons of analytical and numerical solutions for $\alpha=0.1$. (a) the maximum ratio of the base acceleration to the ground acceleration. (b) the maximum ratio of the roof acceleration to the ground acceleration.

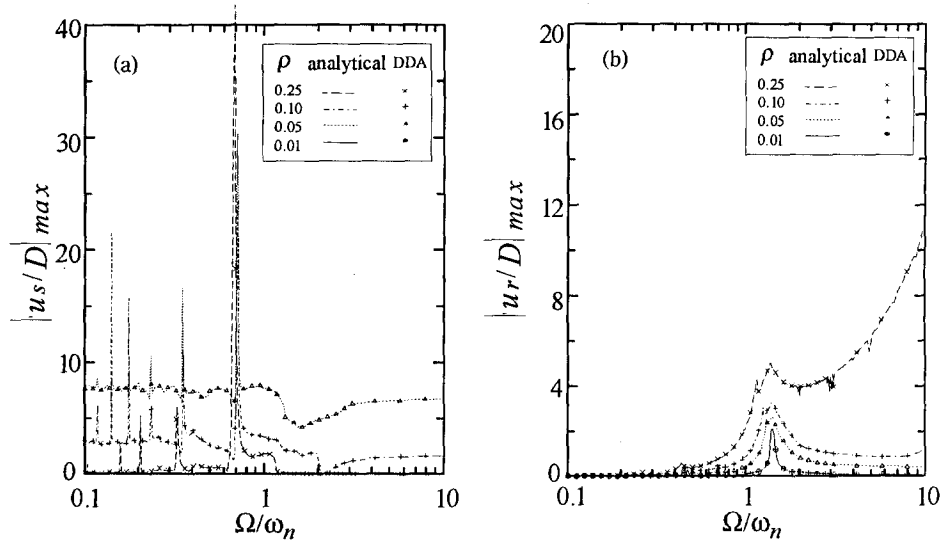


Fig. 6 Comparisons of analytical and numerical solutions for $\alpha=0.5$. (a) the maximum relative displacement between the base and the ground. (b) the maximum relative displacement between the roof and the base.

factor $D=a_{max}/\Omega^2$. For Figs. 5, 7 and 9, each figure has comparisons of the other two measurements: (a) the maximum ratio of the base acceleration to the ground acceleration $|a_{base}/a_{ground}|_{max}$ and (b) the maximum ratio of the roof acceleration to the ground acceleration $|a_{roof}/a_{ground}|_{max}$.

All the comparisons shown in Figs. 4 to 9 indicate that the DDA method can generate reliable answers for simple model simulation. In the following, the DDA model is further used to analyze the three-story structure subjected to a seismic loading. The configuration of the structure is

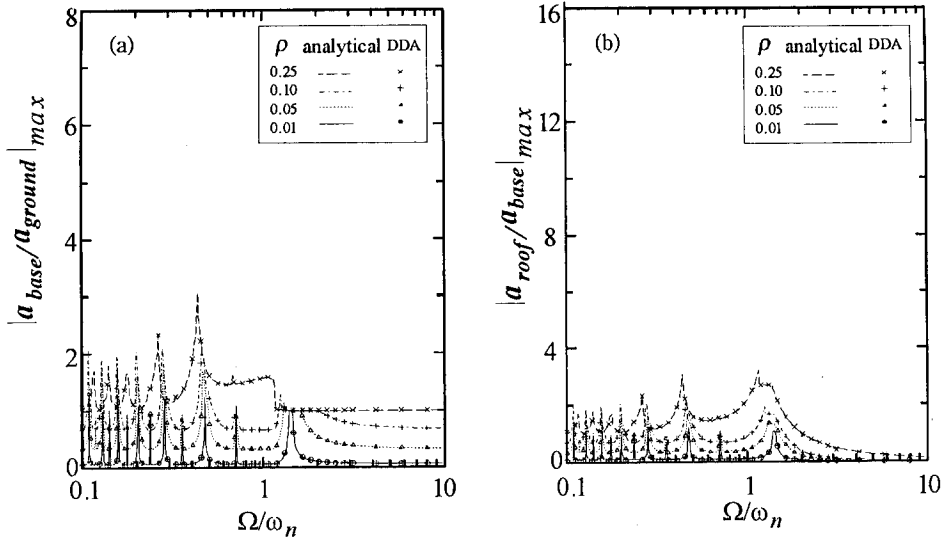


Fig. 7 Comparisons of analytical and numerical solutions for $\alpha=0.5$. (a) the maximum ratio of the base acceleration to the ground acceleration. (b) the maximum ratio of the roof acceleration to the ground acceleration.

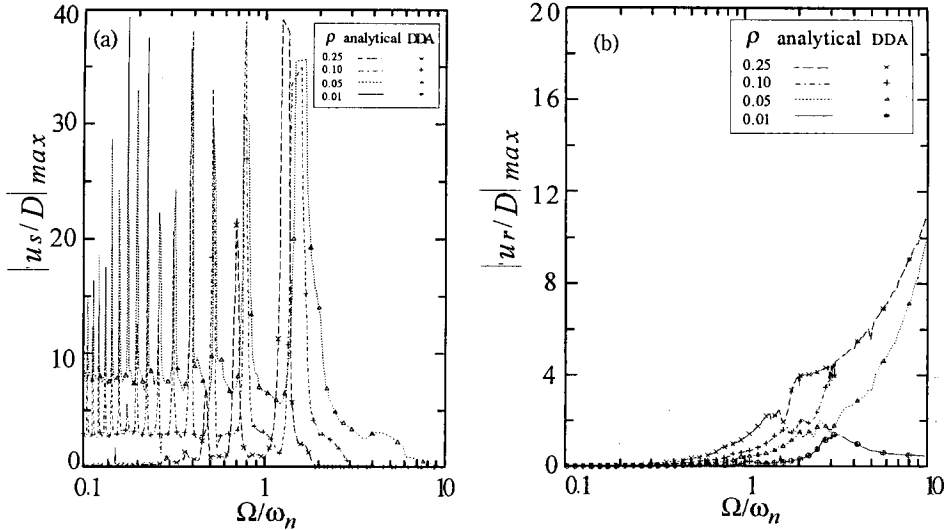


Fig. 8 Comparisons of analytical and numerical solutions for $\alpha=0.9$. (a) the maximum relative displacement between the base and the ground. (b) the maximum relative displacement between the roof and the base.

directly meshed by discrete elements. The mesh and dimensions of the structure are shown in Fig. 3. Triangular connection elements are used wherever the connection is needed. The Young's modulus and the Poisson's ratio of the element's material are 2.0×10^7 kpa and 0.15, respectively. Natural frequencies of the structure for the first three modes are 0.638 Hz, 1.788 Hz and 2.583 Hz. For the sliding phase, frictional coefficient (ρ) of the sliding joint is chosen as 0.01. For the non-sliding (or fixed) phase, the stiffness for both the normal and shear springs used to represent the contact of sliding joint is as 2.0×10^9 kN/m. Acceleration time history of the 1940

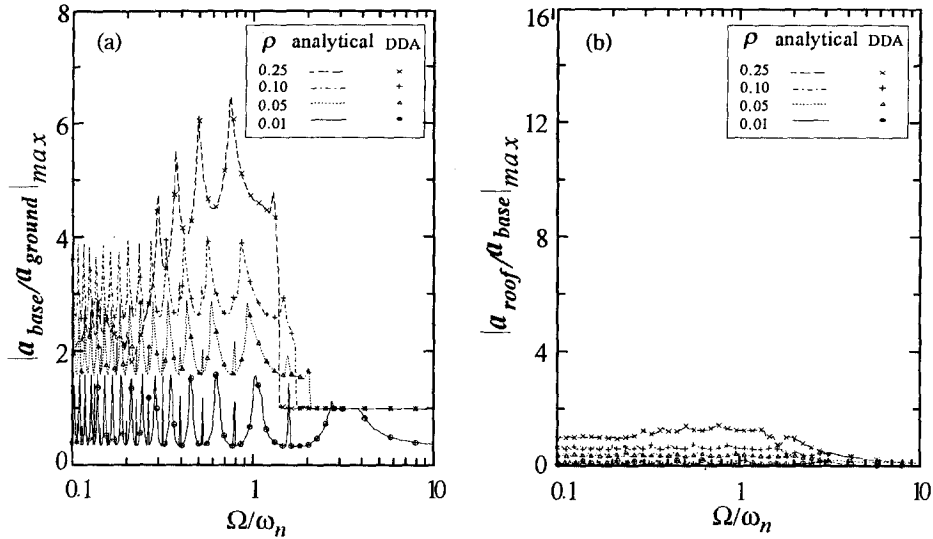


Fig. 9 Comparisons of analytical and numerical solutions for $\alpha=0.9$. (a) the maximum ratio of the base acceleration to the ground acceleration. (b) the maximum ratio of the roof acceleration to the ground acceleration.

El Centro earthquake with time increment of 0.001 second (Fig. 10) is the seismic input. Fourier spectrum of the chosen seismic input is shown as Fig. 11, in which the predominant frequency is about 1.5 Hz. Structural responses under two different conditions, sliding-base and fixed-base, are computed for comparisons.

As can be seen in Fig. 12, the computed sliding of the structure under the seismic ground excitation is presented in the form of the relative displacement of the base to the ground, in which the maximum slip during the excitation is about 0.3 m. At the end of the excitation, the structure displaces about 0.18 m from its origin. Comparing to the chosen El Centro earthquake record (Fig. 10), the seismic excitation which is exerted on the sliding structure from the base through the sliding joint is very limited (Fig. 13). In Fig. 14, the Fourier spectrum of the sliding base excitation indicates that the response predominant frequency is about 0.35 Hz. Comparing to the frequency of 1.5 Hz for the chosen El Centro earthquake record, the predominant frequency of input motion for the sliding structure has been significantly reduced, and is below the natural frequency of the structure itself. For the fixed-base condition, responses of the structure at the roof are presented in Figs. 15 and 16, in which the time history of the roof acceleration and the relative displacement of the roof to the base are shown, respectively. On the other hand, with $\rho=0.01$ for the sliding-base condition, the acceleration of the roof vibration reduces to about one hundredth (Fig. 17), and the amplitude of the vibration is also obviously decreased (Fig. 18). The decrease of both the acceleration and the amplitude of the roof vibration indicates that the sliding base can successfully isolate the structure from a severe ground excitation. The effectiveness of using the sliding base to avoid damaging earthquake is shown by not only the limit acceleration exerted on the structure, but the similarity of accelerations for the base and the roof (Figs. 13 and 17). The shown results reveal that the structure behaves with very little deformation (Fig. 18).

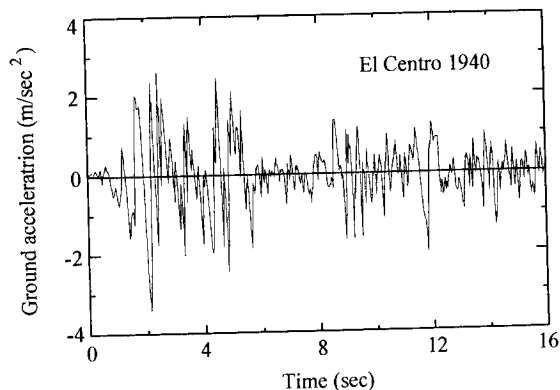


Fig. 10 Acceleration time history of the El Centro earthquake motion.

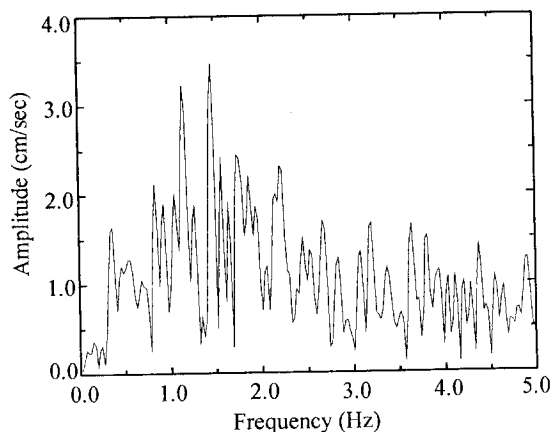


Fig. 11 Fourier spectrum of the El Centro earthquake motion.

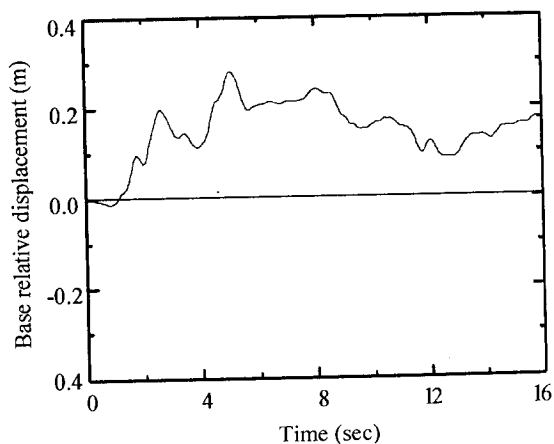


Fig. 12 Relative displacement of the base to the ground ($\rho=0.01$).

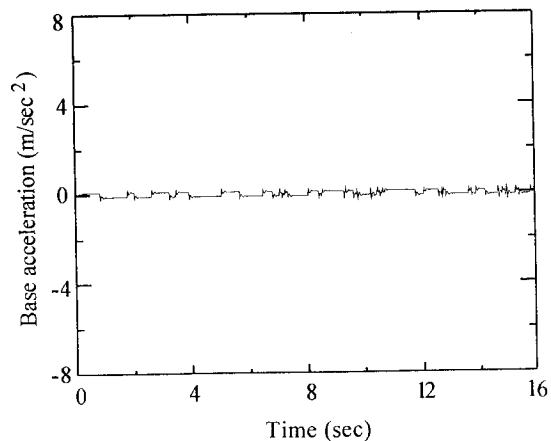


Fig. 13 Base acceleration of the sliding structure ($\rho=0.01$).

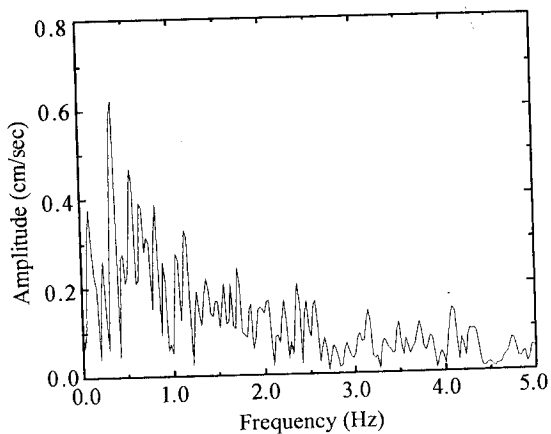


Fig. 14 Fourier spectrum of the base excitation for the sliding structure.

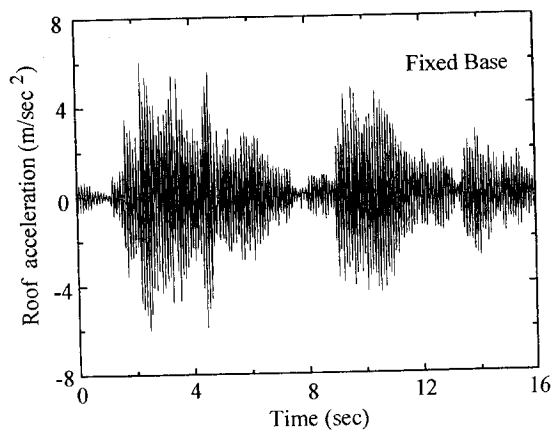


Fig. 15 Roof acceleration of the fixed-base structure.

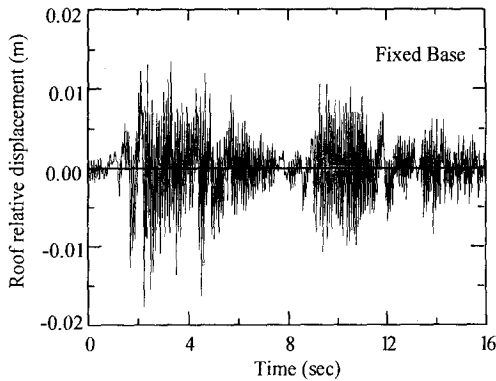


Fig. 16 Relative displacement of the roof to the base for the fixed-base structure.

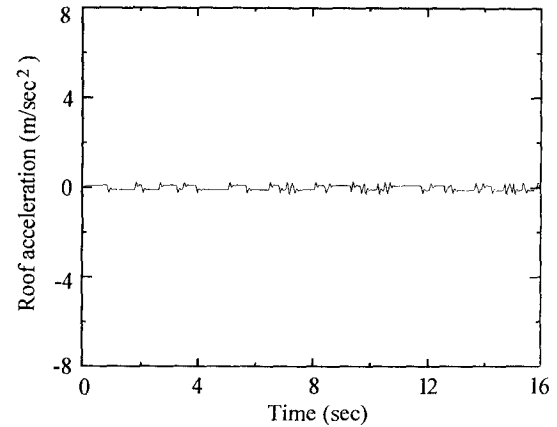


Fig. 17 Roof acceleration of the sliding structure ($\rho=0.01$).

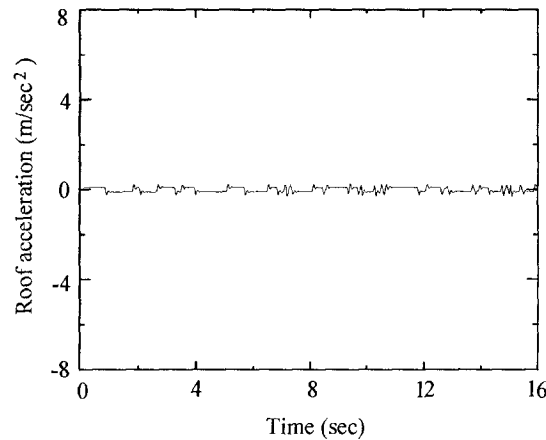


Fig. 18 Relative displacement of the roof to the base for the sliding structure ($\rho=0.01$).

4. Conclusions

The effectiveness of applying a sliding base in reducing the peak responses of structures has been studied using the discontinuous deformation analysis method. This study shows that using this method can simulate the dynamic response of a sliding structure with frictional cut-off quite accurately.

Computations for a simple two-element mass-spring system indicate that results obtained using the DDA model have similar accuracy as those of the analytical solutions using the idealized mass-spring model. Seismic response analysis for a three-story structure with a sliding base reveals that the sliding interface can reduce the ground acceleration or the seismic loading exerted on the structure. This study shows that, for instance, sliding base with frictional coefficient of 0.01 will successfully eliminate the most severe excitation which may be exerted on the structure. The sliding structure may therefore behave with very little deformation. Nevertheless, an irrecoverable displacement for the structure may exist after the seismic excitation.

Appendix I: Formulations of mass-spring model

Using lumped masses (m_N) on a sliding base (m_b), a mass-spring model (Fig. 19) is usually adopted to represent a sliding shear-resistant building of single or multi-degree-of-freedom subjected to a horizontal excitation. Frictional effect along the sliding base is simulated using a fictitious spring. Different spring constants are introduced for sliding and non-sliding phases. In early SDOF models, the spring is modeled in rigid-plastic behavior (Westermo and Udwadia 1983), while it has been improved as an elasto-plastic spring in a more recent MDOF model (Yang *et al.* 1990). The usage of fictitious spring simply avoids the difficulty of solving a sliding boundary problem, and the number of equations remains the same in either the sliding or non-sliding phase. Similar to a typical structural dynamic problem, the equation of motion for typical mass-spring sliding model is

$$[M] \{\ddot{u}\} + [C] \{\dot{u}\} + [K] \{u\} = \{P\} \quad (8)$$

where $[M]$ is the mass matrix, $[C]$ is the damping matrix and $[K]$ is the stiffness matrix, and $\{u\}$ and $\{P\}$ are displacement and external loading vectors, respectively. It should be mentioned that the stiffness matrix with the fictitious spring is as

$$[K] = \begin{bmatrix} k_1 & -k_1 & 0 & \cdots & 0 & 0 \\ & k_1+k_2 & -k_2 & & 0 & 0 \\ & & k_2+k_3 & & 0 & 0 \\ & & & \ddots & \vdots & \vdots \\ & & & & -k_{N-1} & \vdots \\ \text{symm.} & & & & k_{N-1}+k_N & -k_N \\ & & & & & k_N+k_f \end{bmatrix} \quad (9)$$

where k_f is the fictitious spring constant. According to Yang, *et al.* (1990), this constant is a chosen large number for the non-sliding phase and is zero for the sliding phase. The horizontal seismic loading is described as

$$P_i = \begin{cases} -m_N u_0 & i=N \\ -m_b u_0 & i=N+1 \end{cases} \quad (10)$$

Analytical solutions can be derived using the mass-spring model. For instance, as shown in Fig. 2, a single-degree-of-freedom structure of mass m and stiffness k supported by a base raft M that can slide horizontally is chosen to illustrate the theoretical derivation in follows. In this figure u_0 , u_M and u_m are the displacements in an absolute frame of reference, the base raft and the roof, respectively, u_r is the sliding displacement of the base raft relative to the ground, and u_r is the displacement of the roof relative to the base raft. The coefficient of sliding friction is ρ . If the structure slides under the ground excitation, under Newton's second law, the equations of dynamic equilibrium are:

$$m\ddot{u}_m + ku_r = 0 \quad (11)$$

$$M\ddot{u}_M = F - m\ddot{u}_m \quad (12)$$

where F is the friction force mobilized in-between the base-raft and the ground. The maximum value of F during sliding is

$$F = \delta \rho (m + M) g \quad (13)$$

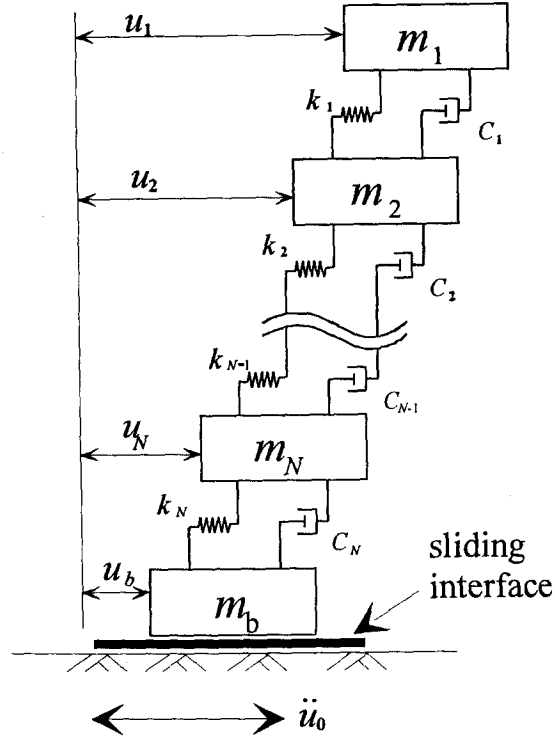


Fig. 19 Mass-spring model.

where δ is either $+1$ or -1 depending on the sign of the velocity, i.e., $\delta = \pm \text{Sgn } \dot{u}_s$. This is a coincidence between the direction of response inertia of the structure and the direction of the ground acceleration. As $\delta = +1$, they are in opposite directions.

Using the relationships of the displacements defined above, Eqs. (11) and (12) can be reformulated as

$$(\ddot{u}_r + \ddot{u}_s + \ddot{u}_0) - \omega^2 u_r = 0 \quad (14)$$

$$\ddot{u}_s = \delta \rho g - \alpha \ddot{u}_r - \ddot{u}_0 \quad (15)$$

where α is the mass ratio and is equal to $m/(M+m)$. Substituting for u_s from Eq. (15) into the equilibrium equation Eq. (14), it can be shown that during the sliding phase

$$\ddot{u}_r + \omega^2 u_r = -\delta \rho g + \alpha \ddot{u}_r \quad (16)$$

$$(1 - \alpha) \ddot{u}_r + \omega^2 u_r = -\delta \rho g \quad (17)$$

$$\ddot{u}_r + \omega_a^2 u_r = \frac{-\delta \rho g}{1 - \alpha} \quad (18)$$

where $\omega_a = \frac{\omega}{\sqrt{1 - \alpha}}$. The solution for the sliding phase is thus obtained by solving Eq. (18) when

$$\rho g - |\alpha \ddot{u}_r + \ddot{u}_0 + \ddot{u}_s| = 0 \quad (19)$$

On the other hand, in the non-sliding phase, $u_s=0$ and the ground moves with an acceleration $\ddot{u}_0=a \sin \Omega t$, Eq. (14) thus becomes

$$\ddot{u}_r + \omega^2 u_r = -a \sin \Omega t \quad (20)$$

The solution for the non-sliding phase can be obtained by solving Eq. (20) when

$$\rho g - |a \ddot{u} + \ddot{u}_0| > 0 \quad (21)$$

The incremental dynamic analysis for solving the above equations can be performed by following the algorithm of Mostaghel, *et al.* (1983b). It is assumed that the structure is in equilibrium at the time step for each increment. Transition of starting and end times of the sliding and non-sliding phases can be obtained as the solution process progresses.

References

- Cundall, P. A. and Strack, O. D. L. (1983), "Modeling of microscopic mechanics in granular material." *Mechanics of granular materials: new models and constitutive relation*, J. T. Jenkins and M. Satake, eds., Elsevier, Amsterdam, The Netherlands, 137-149.
- Cundall, P. A. (1971), "A computer model for simulating progressive, large scale movements in blocky rock systems." *Symposium of International Society of Rock Mechanics*, Nancy, France, 11-18.
- Goodman, R. E., Taylor, R. and Brekke, T. L. (1968). "A model for the mechanics of jointed rock." *Journal of Soil Mechanics & Foundations Division, ASCE*, **94**, 637.
- Li, Z., Rossow, E. C. and Shah, S. P. (1989), "Sinusoidal forced vibration of sliding substructure." *Journal of Structural Engineering, ASCE*, **115**, 1741-1755.
- Mostaghel, N., Hejazi, M. and Tanbakuchi, J. (1983a), "Response of sliding structures to harmonic support motion." *Earthquake Engineering and Structural Dynamics*, **11**, 355-366.
- Mostaghel, N. and Tanbakuchi, J. (1983b), "Response of sliding structures to earthquake support motion." *Earthquake Engineering and Structural Dynamics*, **11**, 729-748.
- Shi, G. H. and Goodman, R. E. (1984), "Discontinuous Deformation Analysis." *Proceedings 25th U. S. Symposium on Rock Mechanics*, 269-277.
- Westermo, B. and Udawadia, F. (1983). "Periodic response of a sliding oscillator system to harmonic excitation." *Earthquake Engineering and Structural Dynamics*, **11**, 135-146.
- Walton, O. R. (1993), "Numerical simulation of inclined chute flows of monodispersed, inelastic, frictional spheres." *Mechanics of Materials*, **16**, 239-247.
- Yang, Y.-B., Lee, T.-Y. and Tsai, I.-C. (1990), "Response of multi-degree-of- freedom structures with sliding supports." *Earthquake Engineering and Structural Dynamics*, **19**, 739-752.